MACHINE-HUMAN INTERACTIONS

Motor learning affects car-to-driver handover in automated vehicles

Holly E. B. Russell,[1] Lene K. Harbott,[1]* Ilana Nisky,[2] Selina Pan,[1] Allison M. Okamura,[1] J. Christian Gerdes[1]

Vehicles in the foreseeable future will be required to transition between autonomous driving (without human involvement) and full human control. During this transition period, the human, who has not been actively engaged in the driving process, must resume the motor control necessary to steer the car. The in-car study presented here demonstrates that when human drivers are presented with a steering behavior that is different from the last time they were in control, specifically the ratio of hand wheel angle to road wheel angle (emulating a change in vehicle speed), they undergo a significant period of adaptation before they return to their previous steering behavior. However, drivers do not require an adaptation period to return to previous driving behavior after changes in steering torque. These findings have implications for the design of vehicles that transition from automated to manual driving and for understanding of human motor control in real-world tasks.

INTRODUCTION

A transformation in human transit and mobility is fast becoming realized through technological advances in automated vehicles, with more and more of the driving responsibility transferred from the human to the car. To date, the most advanced systems offered for sale in automobiles are what the SAE International's J3016 standard characterizes as level 2 or partial automation systems (*1*). Such vehicles automate steering and acceleration/deceleration in specific driving modes but require the driver to remain in the control loop and retain responsibility for driving. The next stage of automation (level 3 or conditional automation) envisions vehicles that transition between automated driving (without human involvement) and full human control, depending on the situation (*1*). Level 3 automated vehicles may request a transition of control from the vehicle to the human, initiating a transition period that requires the driver, who has not been actively engaged in the driving process, to reacquire the situation awareness needed to navigate the road environment and to physically resume the motor control necessary to steer the car. Although the issue of drivers regaining situation awareness during handover in automated driving has received substantial recent attention (*2*–*4*), the motor control implications of a rapid, and possibly unanticipated, transition from fully automated to fully manual driving have not been explored (*5*).

Laboratory studies of human motor control and learning provide a wealth of evidence about how we coordinate movements and adapt to novel situations by processing sensory information, updating internal model representations, and computing control commands (*6*–*8*). The motor system uses feedback and feedforward mechanisms to coordinate movement (*9*, *10*) and adaptation to continually update the internal model on which the feedforward mechanism relies. The speed and extent to which a person adapts depend on many factors, including the amount of perturbation (*11*, *12*), the error experienced and its history (*13*–*16*), and the type of feedback received (*17*, *18*). Careful experimental design can help in identifying the variables that are used by the motor system to construct the internal representations (*19*) and how they are represented (*20*, *21*). The nature of human motor control is subject to active computational, behavioral, and imaging research, but many questions remain (*10*). Specifically, it is not well understood how theories extend to real-life situations outside the laboratory environment (*22*, *23*), and especially to driving a vehicle, where the driver controls the vehicle while receiving a multitude of sensory signals, including visual information of the road, proprioceptive information of the steering wheel angle, haptic information of the steering wheel resistance, and the inertial forces resulting from linear and angular acceleration of the vehicle.

Steering is a complex motor control task that relies on the driver having an accurate internal model of how steering commands map to vehicle dynamics (*24*), in particular rotational velocity (yaw rate). This model varies with the speed of the car, and in the case of handover from an autonomous controller to a human driver, there is no guarantee that the human driver retakes control at the same vehicle speed at which control was relinquished. We hypothesize that this situation would result in the driver relying on an incorrect internal model immediately upon retaking control and requiring some period of time to adapt to the new driving situation to achieve their previous driving performance under the new circumstances.

RESULTS

To investigate whether such an adaptation period exists, and how steering behavior changes during adaptation, we designed an experimental lane change task to be driven in an electric, steer-by-wire car (Fig. 1A) while the steering properties of the car were modified. The lane change task required the driver to steer the vehicle down the center lane of the course as it automatically accelerated to a speed of 8 m/s (fig. S3), make a single lane change right or left as indicated by a signal light in the driver's direct line of sight (Fig. 1A, lower right, and fig. S4), and come to a stop in one of two target gates (Fig. 1B). The direction of the lane change was pseudorandomized for each trial. Between trials, the vehicle autonomously steered back to the start of the course (fig. S5) so that the beginning of each trial represented a handover of steering control between the automated vehicle and the driver.

Each participant drove four baseline trials with steering ratio and steering torque values similar to those used in most modern production vehicles. This was followed by 10 perturbation trials, where one of

[1]Department of Mechanical Engineering, Stanford University, Stanford, CA 94305, USA. [2]Department of Biomedical Engineering and Zlotowski Center for Neuroscience, Ben-Gurion University of the Negev, Beer Sheva 8410501, Israel.
*Corresponding author. Email: lharbott@stanford.edu

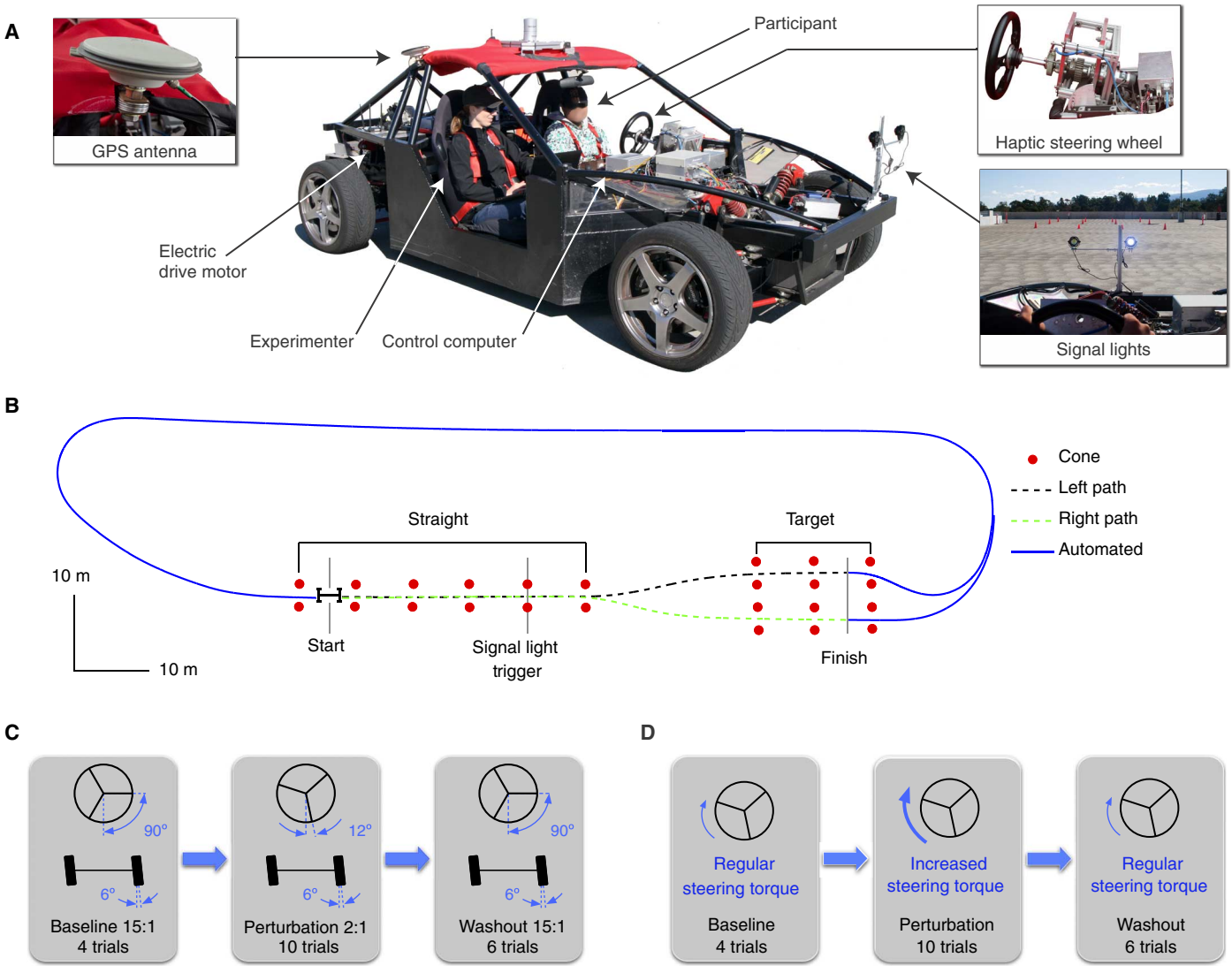

Fig. 1. Experimental setup. (**A**) The experimental vehicle used in this study is X1 (*37*) with inset views of the GPS antennas, the haptic steering wheel system, and the lights that signal the lane change direction in each trial (as depicted, indicates that the driver must make a right lane change). (**B**) The driving course was marked with traffic cones. The lane change direction was signaled shortly before the end of the straight section, and the black and green paths represent example left and right lane changes, respectively. The blue lines depict the paths the vehicle automatically followed between trials. (**C**) For the steering ratio change, the steering ratio was 15:1 during the baseline and washout trials, meaning that the driver must turn the steering wheel 90° for the road wheels to turn 6°; during the perturbation trials, a 2:1 steering ratio reduced the steering wheel motion to 12° for the same 6° at the road wheels. (**D**) For the steering torque change, participants experienced baseline steering torque during the baseline and washout trials, and the torque was increased during the perturbation trials. (C and D) The study protocol consisted of 4 baseline, 10 perturbation, and 6 washout trials.

two steering properties was modified: Either the steering ratio was reduced from 15:1 to 2:1 (steering wheel angle/road wheel angle) to simulate the change in vehicle dynamics that drivers would experience when transitioning from parking lot speed (~9 mph) to highway speed (~67 mph) or the steering wheel torque was increased by a factor of about 2.3 through a nonlinear steering feel controller (figs. S1 and S2) to simulate how the steering feel would change when transitioning from driving with power steering to driving without power steering. Last, participants completed six washout trials with baseline steering properties to investigate washout of learning (Fig. 1, C and D). For safety considerations, participants were notified before the first perturbation and the first washout trials regarding the nature of the change in the steering properties that they were about to experience. Each trial took about 15 s to complete. A total of 22 licensed drivers participated in the study, with 10 experiencing the steering ratio change and 12 undergoing the steering torque modification.

Example data of road wheel angle versus distance along the path for two representative participants during the baseline trials (Fig. 2, A and C, green) show steering profiles consisting of a large change in wheel angle to make the initial lane change, followed by a smaller steering movement to straighten the car relative to the target gate. Perturbing the steering ratio from 15:1 to 2:1 (Fig. 2A, blue) resulted in the driver making many steering oscillations to successfully complete the lane change task, with progressive reduction in the oscillatory behavior over the perturbation trials. In addition, the first local maximum steering angle following the signal light trigger (denoted

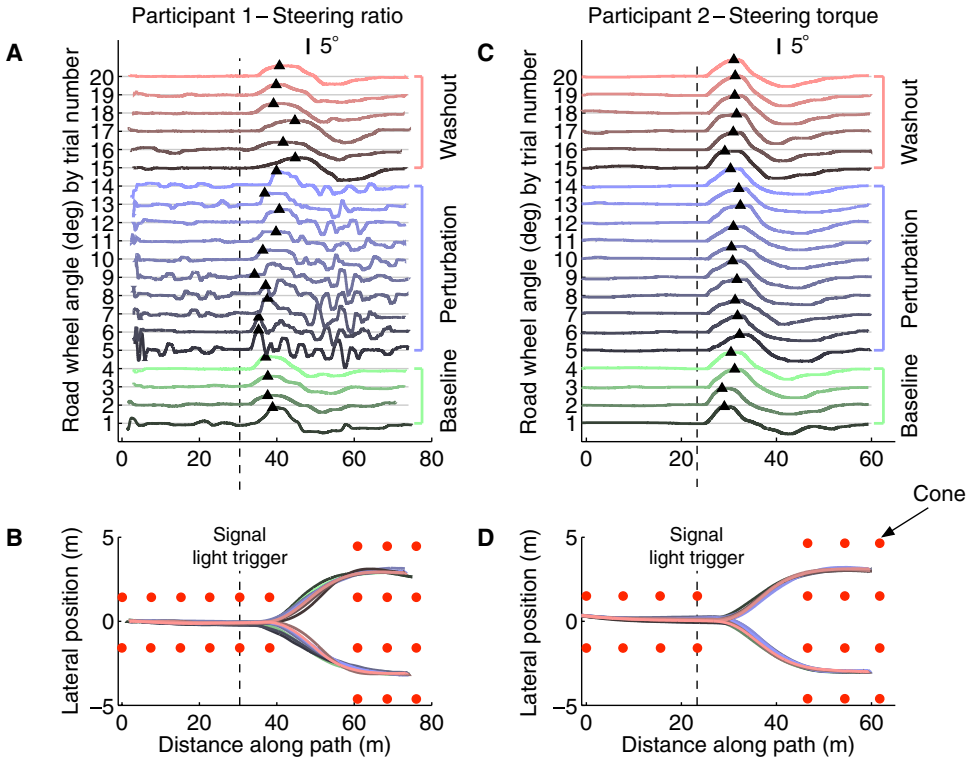

Fig. 2. Perturbing steering ratio resulted in markedly different steering profiles during a lane change; steering profiles remained consistent for perturbed steering wheel torque. (**A** and **C**) Road wheel angle versus distance along the path during the steering task for all 20 trials for one representative participant for each steering change. Zero road wheel angle is indicated for each trial by a light gray line. For visualization purposes, road wheel angles in right lane changes are mirrored for a left lane change, although participants performed an equal number of left and right lane changes. Triangles indicate local maximum steering angles. During baseline trials (1 to 4), both participants used smooth steering motions to make the lane change. When steering ratio was perturbed in adaptation trials (5 to 14), participant 1 showed increased oscillations in road wheel angle, whereas participant 2 maintained consistently smooth steering motions when steering torque was perturbed. Both participants used smooth steering motions during washout trials (15 to 20). (**B** and **D**) Paths taken by the vehicle during each trial (for visualization purposes, vertical and horizontal axes have different scales). Although straight course sections had different lengths due to experimental facility availability, the distance from the end of the straight to the target gates was consistent.

by triangles) occurred earlier in the path compared with baseline. On removal of the perturbation (Fig. 2A, red), the steering behavior recovered the shape that was seen in the baseline trials; the timing of the steering peak shifted later than baseline. In contrast, perturbing the steering torque (Fig. 2B) did not induce an obvious change in steering profile, except for a slight variability in the timing of the steering peak. The paths taken by the vehicle were more consistent for the torque perturbation (Fig. 2D) compared with the steering ratio perturbation (Fig. 2C), although both participants successfully completed all trials while staying within the course boundaries.

The data in Fig. 2 were quantified for the entire group of participants using three metrics. First, steering reversal rate counts the number of times per second the steering wheel changes direction through an angle of at least 0.5°; high steering reversal rates have been correlated with increased steering task difficulty (*25*). Second, root mean square (RMS) steering speed measures the average speed of steering motions over the course of a full trial, with higher values representing increased steering control input necessary to complete the lane change. Both the metrics of steering reversal rate and RMS steering speed quantify the feedback responses that drivers use to compensate for errors in vehicle steering, so they can successfully complete the lane change task (*9*). However, neither is primarily a measure of feedforward control, as corroborated by the absence of an aftereffect in these metrics upon removal of the perturbation. The third metric, time to steering peak, measures the elapsed time between triggering the lane change signal light and the next local maximum steering angle. This measure not only includes reaction time and feedback components, but, most importantly, is strongly affected by the feedforward component of the driver's motor control. The feedforward component uses an internal model to plan the actions necessary for turning the steering wheel with a timing that enables a comfortable lane change. After a perturbation occurs in the steering input (such as a steering ratio decrease), the driver's internal model is initially wrong—this leads to an overshoot in the vehicle motion if the driver uses the initial steering motion planned based on the erroneous internal model. Similarly, when the perturbation is removed, the newly learned internal model is once again incorrect and results in an undershoot.

Average steering data for all participants are shown in Figs. 3 and 4. Immediately after perturbation of the steering ratio, the steering behavior deviated significantly from the previous behavior seen in the baseline trials, illustrated by the significant increase in steering reversal rate and steering wheel speed and significant decrease in time to steering peak between trials 4 and 5 (Figs. 3, A to C, and 4, A to C). All three measurements of driver steering behavior then gradually returned to baseline levels within 10 trials.

Motor learning studies typically demonstrate learning by presenting a reduction in performance error and/or an increase in movement speed (*22*, *23*). In our experiment, we cannot quantify an error or vehicle speed measurement for each trial. This is because, in our paradigm, there are many possible driving trajectories, and thus many possible sequences of steering commands, that allow successful completion of the lane change task, and the vehicle is travelling at a constant velocity. Instead, by quantifying the driver's steering commands, we show a clear learning curve as drivers initially react to a change in steering ratio by modifying their steering behavior significantly from original, baseline behavior, and then demonstrate a period of adaptation, during which their steering behavior returns to baseline levels, despite the perturbed steering ratio.

When the steering ratio perturbation was removed, drivers' steering behavior showed a clear aftereffect, because the average time to steering peak occurred significantly later than during the baseline trials (Figs. 3C and 4C). The metrics of steering reversal rate and average steering speed do not capture any aftereffect; upon return to baseline steering ratio, a driver turning the steering wheel too little to command the

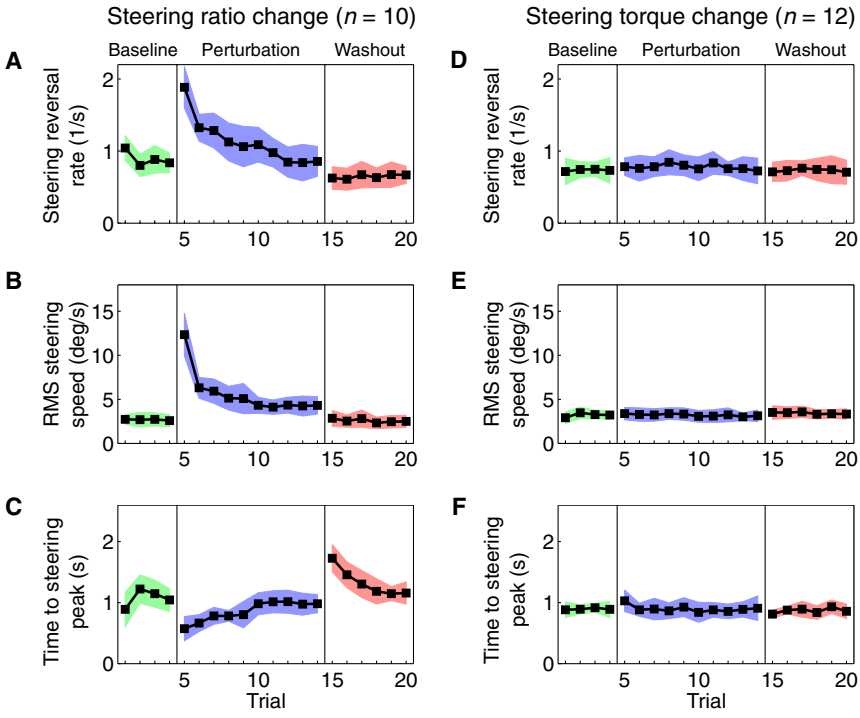

Fig. 3. Perturbation of steering ratio demonstrates adaptation effects in drivers. Left: Three metrics versus trial number averaged across participants for steering ratio scaling study (symbols are means, shaded regions indicate 95% confidence intervals calculated using a *t* distribution): (**A**) steering wheel reversal rate, (**B**) RMS steering speed, and (**C**) time from signal light trigger to first local maximum steering angle. Right: Same three metrics for the steering torque study: (**D**), (**E**), and (**F**), respectively. There are clear learning curves during the perturbation phase for the steering ratio study (A to C), with aftereffect in the elapsed time metric (C; washout section). In contrast, all three metrics show very little change throughout baseline, perturbation, and washout phases for the steering torque change.

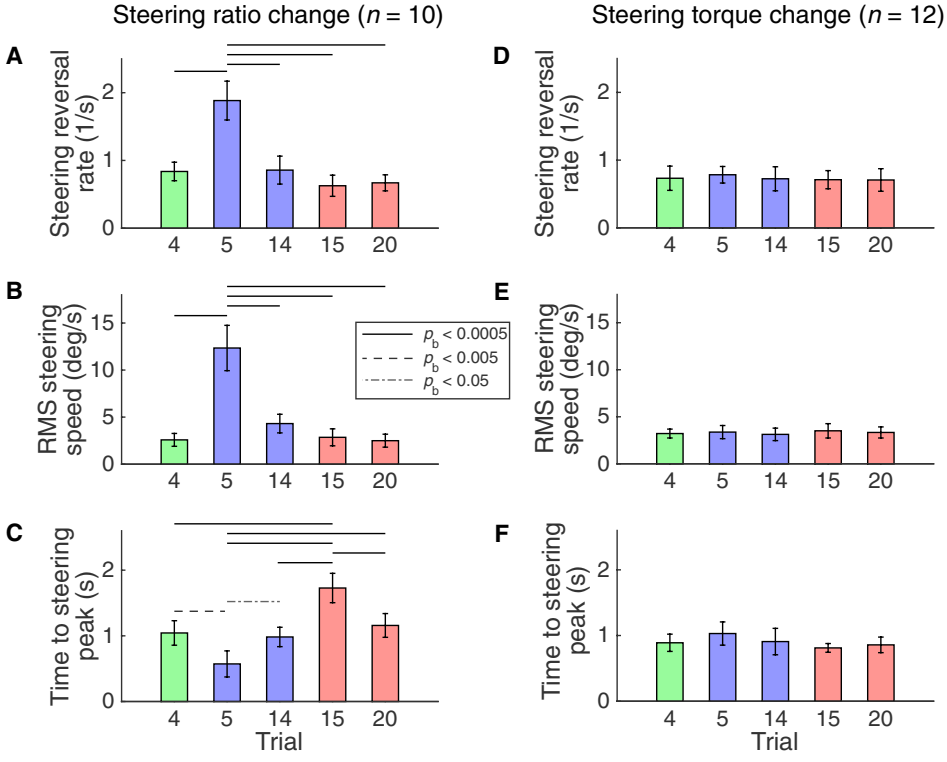

Fig. 4. Motor learning effects are statistically significant for steering ratio change but not for steering torque change. The three metrics for each modification were averaged across participants for the last baseline trial (*4*), the first (*5*) and last (*14*) perturbation trials, and the first (*15*) and last (*20*) washout trials. Left: Results for steering ratio change: (**A**) steering wheel reversal rate, (**B**) RMS steering speed, and (**C**) time from signal light trigger to first local maximum steering angle. Right: Same metrics for steering torque change: (**D**), (**E**), and (**F**), respectively. Bars indicate estimated means, and error bars indicate 95% confidence intervals calculated using a *t* distribution. Horizontal lines indicate statistically significant post hoc comparisons with a Bonferroni correction for multiple comparisons (thus, all *P* values are corrected by multiplying by 10), following a repeated-measures one-way ANOVA, at the $\alpha = 0.05$ significance level. All the *P* values for the *F* tests and post hoc *t* tests are specified in the Supplementary Materials (tables S1 to S3).

planned vehicle response needs only to increase the angle, rather than perform a steering reversal, or increase their steering speed. This absence of an aftereffect suggests that these metrics primarily quantify feedback and not feedforward components of control.

Unlike many motor adaptation studies to date, participants were told before a change in the steering/torque ratio. This is consistent with the idea that, in handover situations, the drivers will be aware that they are retaking steering control. Being informed of the change in the steering/torque ratio, the participants very likely used explicit adjustments to cope with the perturbation, especially in the washout (*26*). However, the existence of aftereffects indicates that an implicit process, of which the participants were unaware, was part of the adaptation.

Most modern passenger vehicles have a steering ratio on the order of 15:1, so the drivers in this study have substantial experience of the baseline steering ratio. The drivers fully adapt to a marked change in steering ratio within only 10 trials. Results show that participants sufficiently update their internal model of the vehicle's response to their steering commands such that a clear aftereffect is observed upon return to the familiar steering ratio, although they were informed before the first washout trial that the car would return to normal steering. Adaptation over this limited number of trials may seem unusual, but the driving task presented here is very different from most of the previously published studies of motor adaptation. For example, in arm reach adaptation after a visuomotor rotation (*8*) or a force field perturbation (*27*), a typical trial lasts less than a second and typically includes a single ballistic feedforward-controlled movement with feedback corrections at the end of the movement. Our trials last 15 s, and the driver could probe the system with minor penalty while driving on the straight portion of the track, before steering to make the lane change (see the steering profiles to the left of the dashed line in Fig. 2A). This makes the disassociation between feedforward and feedback components of control in our driving task, and in the metrics that quantify adaptation, particularly challenging. The amount and modality of the sensory feedback that the driver receives also differ from reach studies: In the current paradigm, the drivers experience the vehicle dynamics by their entire body, whereas in classical reach studies participants receive only proprioceptive feedback of the arms and visual feedback of cursor location. Despite these many differences from classical motor control studies, our results of adaptation and aftereffect suggest that there are global mechanisms of motor learning that take place when the motor system encounters a novel situation.

Perturbing the steering torque did not result in significantly different steering reversal rate, steering speed, or time to local maximum steering peak (Figs. 3, D to F, and 4, D to F). The steering torque perturbation did not prevent drivers from successfully making the lane change, suggesting that our metrics are insensitive to the adaptation to a change in steering torque. It is likely that the drivers responded to the torque perturbation very quickly by modifying the impedance of their arms by co-contraction of their arm muscles (*28*). Although the magnitude of the steering torque perturbation is less than that of steering ratio change, driving simulator experiments have demonstrated that drivers react to steering torque changes by modifying the co-contraction of their arm muscles to stiffen their arms (*29*, *30*), consistent with our current findings on the drivers' measured steering behavior.

DISCUSSION

The results presented here suggest that designers of automated vehicles need to consider a period of significantly different steering behavior as drivers adapt to differences in the relationship between steering angle and vehicle motion that have occurred before handover. We show that drivers adapt to a change in steering angle by changing their steering behavior, suggesting that steering angle is the fundamental variable on which drivers base their steering control. In contrast, drivers' steering behavior is robust to changes in steering torque (*30*, *31*), likely due to rapid increase in the mechanical impedance of their arms by means of muscle co-contraction. This suggests that changes of steering torque are of lesser importance in the design of safe car-to-driver handover.

Although this experiment was not designed to explicitly measure the total time required to adapt to the steering change, the results indicate that the adaptation process took place over more than a minute. Drivers could still complete the lane change even with the large change in steering ratio, but their performance as measured by the steering metrics was compromised while they adapted to the change. In addition to concluding that driver performance in a single lane change steering task is compromised, we hypothesize that the ability of drivers to safely respond to any additional hazard during this adaptation period would be similarly affected. Furthermore, we anticipate that the effects of additional cognitive load, such as the mental effort required to follow driving directions or talk to a passenger, would have detrimental effects on adaptation to altered steering. Therefore, these results suggest that designers of automated vehicles should carefully consider this period of compromised steering behavior when choosing methods for handover of control and conduct extensive experimentation with a wide range of a representative population of drivers in their design process. One promising alternative to sudden, discrete handover is the concept of shared control, where the vehicle and the human share control authority (*32*). A period of shared control while the driver regains previous driving skill after a change in steering properties could mitigate the risk associated with the adaptation process.

MATERIALS AND METHODS

Study design

This study was designed to investigate how drivers compensate for changes in steering behavior of a vehicle, by perturbing either the steering ratio or the steering torque of the vehicle. Drivers were instructed to perform a series of single lane change maneuvers under the perturbed steering conditions to determine to what extent drivers can adapt to the novel vehicle control conditions and to investigate which aspects of drivers' steering behavior are modified to successfully complete the lane change tasks during, and after, the adaptation period.

Participants were randomly assigned to one of the experimental groups (a total of 10 participants completed the steering ratio study, and a total of 12 completed the steering torque perturbation study), and every participant experienced the same sequence of experimental trials (4 baseline, 10 perturbation, and 6 washout trials; see Results section for details) to investigate driver adaptation to the perturbation with increasing experience of the novel control conditions. All 22 participants completed all 20 trials, and steering behavior data from all trials and all participants were included in the analysis. For safety reasons, the experimenter (present in the vehicle at all times) and the driver knew which perturbation type the driver would experience in advance of each trial. The data were not blinded for subsequent analysis.

Experimental design

Experimental vehicle

The X1 experimental vehicle was designed and built by students at Stanford University, and is used for a wide range of experiments in vehicle dynamics and control. The drivetrain consists of a 75-kW brushless permanent magnet motor (UQM Technologies Inc.) with 240 N·m of peak torque and an open differential with 7:1 gear reduction (Strange Engineering). The motor is powered by a pack of 28 deep-cycle lead-acid batteries (Optima Batteries Inc.) with a nominal pack voltage of 336 V.

The vehicle is equipped with a dual braking system consisting of two brake calipers on each wheel: one for manual braking and one for electronically controlled braking. The manual brakes use a standard configuration of hydraulic components. With the electronic brakes (TNO), the brake pressure on each wheel can be controlled independently through a hydraulic pump. The maximum pressure for each wheel is 120 bar, and the brake pressure has a rise time of about 100 ms.

The steering is controlled with independent steer-by-wire systems on all four wheels, each consisting of a dc motor (Magmotor), a harmonic drive with gear reduction of 160:1 (Harmonic Drive LLC), a motor controller that communicates via CAN (ADVANCED Motion Controls), and a custom steering linkage. A pack of four lead-acid batteries (EnerSys) with a nominal pack voltage of 48 V provides power for the steering motors. The front wheels are capable of steering to ±23°, whereas the rear wheels can steer to ±14°. A custom-built adjustable steering wheel assembly provides haptic feedback to the driver using a dc motor (Magmotor) and a harmonic drive (Harmonic Drive LLC), providing maximum steering wheel torque of 15 N·m.

Vehicle localization and state measurement are performed with a system that tightly integrates an inertial measurement unit and a Global Navigational Satellite Systems receiver (NovAtel Inc.). The system provides position, velocity, acceleration, and rotational rate information at 100 Hz. The satellite measurements are augmented with OmniSTAR HP differential global positioning system (GPS) corrections (OmniSTAR) to localize the vehicle within about 10 cm and a local GPS reference base station to provide overall position accuracy within 2 cm.

The vehicle has a single control computer to handle all basic vehicle sensing and control, the MicroAutoBox II 1401/1511/1512 (dSPACE GmbH). Control software is designed using Simulink (version R2011a, MathWorks) and operates at 500 Hz. Program execution and data recording are controlled through ControlDesk software (version 7.1, dSPACE GmbH). More than 200 signals are recorded at each execution time step, of which about 20 are relevant to the study of driver adaptation. Data recorded in ControlDesk are exported to MATLAB (version R2011a, MathWorks) for analysis.

Experimental steering task

The experimental task consists of a single lane change at a prescribed speed. The task starts with the vehicle stationary at the beginning of the course (Fig. 1B). The experimenter, sitting in the passenger seat, pushes a button to activate the cruise control system, which accelerates the vehicle up to a maximum speed of about 8 m/s and holds at that speed for the duration of the maneuver. As the vehicle is accelerating, the driver steers the vehicle straight down a 3-m-wide lane bordered by pairs of cones. When the vehicle approaches the end of the straight segment, one of two signal lights on the vehicle's front bumper illuminates to indicate which direction the driver should steer. On the basis of which light is active, the driver steers into the left or right gate, each of which is 3 m wide and demarcated by pairs of cones. As soon as the driver has completed the steering action, he presses the brake to bring the car to a stop before the last pair of cones in the target gate. The lateral (steering) and longitudinal (acceleration and braking) control of the vehicle are separated during the task to standardize the experiment between drivers and to ensure that drivers are primarily focused on the steering task, not on maintaining vehicle speed. The subsystems that make up the steering task are described in more detail below.

Steering ratio and steering torque. In a conventional steering vehicle, there is a fixed relationship between the angle of the road wheels and the angle of the steering wheel (or handwheel) because they are physically connected through the steering shaft. This is often represented as a linear relationship between the handwheel angle δ_{hw} and the road wheel angle δ_f, where the constant is the steering ratio K_{sr}, defined in Eq. 1.

$$\delta_{hw} = K_{sr}\delta_f \tag{1}$$

For a steer-by-wire vehicle such as X1, there is no mechanical connection between the handwheel and the road wheels. This means that the steering ratio can be changed in software to the desired value. Here, for the steering ratio perturbation, $K_{sr} = 15$ for the baseline scenario and $K_{sr} = 2$ for the perturbation stage.

The driver of a conventional vehicle feels torque at the handwheel that communicates information about the tire forces that the vehicle is experiencing. In X1, there is no direct application of steering torque related to the tire forces, so for driver safety and comfort, it is necessary to create an artificial steering feel. This is also used to create the steering torque perturbation for the study. In general, with a force feedback steering system, the handwheel torque τ_{hw} can be modeled as the sum of the torque applied by the motor τ_{motor} and the torque due to the steering system dynamics. A simple version of this model is as follows:

$$\tau_{hw} = \tau_{motor} + b\dot{\delta}_{hw} + J\ddot{\delta}_{hw} \tag{2}$$

where J is the steering system inertia and b is the steering system damping. The designer is free to choose the motor torque to provide the desired steering feel. Two different motor torque models are used for the studies presented here: the linear spring model and the full steering feel emulator.

Linear spring model. For the steering ratio perturbation, the steering motor torque τ_{motor} is computed using the linear spring model, plotted in fig. S1 and described mathematically in Eq. 3.

$$\tau_{motor} = \begin{cases} -\dfrac{1.125\pi}{\delta_{f,max}K_{sr}}\delta_{hw}, & \dfrac{|\delta_{hw}|}{K_{sr}} \le \delta_{f,max} \\ -1.125\pi \mathrm{sgn}\delta_{hw} - 100(\delta_{hw} - \delta_{f,max}K_{sr}\mathrm{sgn}\delta_{hw}), & \dfrac{|\delta_{hw}|}{K_{sr}} > \delta_{f,max} \end{cases} \tag{3}$$

In this model, the torque applied by the handwheel motor is proportional to the handwheel angle δ_{hw}, as long as the road wheel angle δ_f corresponding to δ_{hw} (the relationship shown in Eq. 1) is less than the maximum road wheel angle physically possible, $\delta_{f,max}$ (first case in Eq. 3). Because the vehicle uses steer by wire, the handwheel can continue turning when the road wheels have reached their physical limit, so an artificial "hard stop" is created by applying a large torque through the handwheel motor. This simulated hard stop is the affine function in the second case of Eq. 3 and essentially saturates to a maximum torque of 6 N·m when the handwheel has gone just a few degrees past the linear range.

Full steering feel emulator. For the steering torque perturbation, the handwheel torque is a more complex function that mimics the torque that would normally be observed in a conventional steering car. The full steering feel emulator, developed by Balachandran and Gerdes (*33*) and summarized here, is depicted in block diagram form in fig. S2A. The motor torque for the full emulator is given by the following:

$$\tau_{motor} = \tau_{inertia} + \tau_{damping} + K\tau_{assisted} \tag{4}$$

where $\tau_{inertia}$ and $\tau_{damping}$ are used to modify the effective inertia and damping experienced at the handwheel. The total assisted tire moment $\tau_{assisted}$ models the combination of tire aligning moment $\tau_{aligning}$, tire

jacking torque $\tau_{jacking}$, and power assist. K is a gain that controls how much of the total assisted tire moment is transmitted to the handwheel. The assisted tire moment is modeled with the following equation, where W is a power assist weighting function that depends on the front tire slip angle α and the lower limit parameter γ, as depicted in fig. S2B.

$$\tau_{assisted} = W(\alpha,\gamma)(\tau_{jacking} + \tau_{aligning}) \quad (5)$$

To create the steering torque modification, the weighting function lower limit γ is changed from a baseline level of 0.2 to 1, and the assisted tire moment gain K is increased from 0.03 to 0.05.

Cruise control. To keep the conditions of the experiment consistent across all participants and to focus the driver's attention on the steering task, a cruise control algorithm regulates the vehicle's longitudinal speed. Each trial begins with the experimenter pressing a button to enable the cruise control. When the button is pressed, the desired speed $U_{x,des}$ is gradually increased from 0 to 8 m/s using a two-pole 0.5-Hz discrete low-pass filter, $L_2(z)$.

$$L_2(z) = \frac{3.948 \times 10^{-5}}{z^2 - 1.987z + 0.9875}$$
$$U_{x,des} = 8L_2(z) \quad (6)$$

Given the desired speed, electric drive motor torque τ_m, actual speed U_x, and proportional feedback gain K_{cruise} = 35 N·s, the control algorithm is a simple proportional controller.

$$\tau_m = K_{cruise}(U_{x,des} - U_x) \quad (7)$$

The operation of the cruise control algorithm for a sample experiment is depicted in fig. S3. Because the desired speed smoothly increases over the course of about 1 s, the drive motor torque at first ramps from zero to its maximum value of 240 N·m and then saturates for a couple of seconds. The torque gradually decreases to a steady-state value at around 9 s, and then the driver steps on the brake at about 11 s to disable the cruise control and bring the car to a stop around 14 s.

Signal light trigger. The signal lights are attached to the front bumper of the experimental vehicle, in clear view of the driver as he looks ahead along the path (Fig. 1A). Both lights are off while the vehicle accelerates down the straight segment of the course. As the vehicle nears the end of the straight, one of the lights illuminates to indicate which lane the driver should change into. The condition for activating the signal lights is that the vehicle center of gravity is within a certain range of X values (where X is oriented along the path), as pictured in fig. S4.

The lane change direction for each trial is predetermined by generating a vector of 20 discrete random variables in the set (−1,1), with −1 corresponding to a right turn and 1 corresponding to a left turn. The vector of random variables is adjusted by hand to ensure that there are 10 trials in each direction.

Between-trials return to start

After the driver completes the primary task and brings the vehicle to a stop, the path following controller is activated to bring the vehicle back to the start of the course. During this phase of the experiment, the driver controls the speed of the vehicle with the accelerator and brake pedals while the steering is controlled automatically to track the reference path. This phase is important for two reasons. First, because the driver does not control the steering during this phase, any adaptation to the steering perturbation is confined to the primary task and can be analyzed consistently between participants. Second, the semi-automated nature of this phase mimics a self-driving car, and thus, the experiment addresses a scenario in which a human driver takes over steering control from an automated vehicle.

Map generation. The reference path is designed using a MATLAB program called Quill (fig. S5), developed at Stanford University. The path consists of a set of simple path elements that have curvature that is easy to describe: straight segments (zero curvature), arcs (constant curvature), and clothoids (linearly varying curvature). Each straight segment is followed by an associated set of turn elements: an entry clothoid (increasing curvature), an arc, and an exit clothoid (decreasing curvature). The equations for east position, north position, and heading angle for each type of segment are presented in (*34*).

First, the GPS coordinates of the desired path are measured while driving the vehicle through the course. The path is created in Quill by adding enough straight segments to adequately represent the path and then adjusting the parameters of the turn segments until the calculated path is close enough to the measured path. Adjusting turn parameters entails changing the length of the clothoid segments with respect to the constant radius arc segment. Last, the map data are exported to a CSV (comma-separated values) file that consists of map segments (straights, clothoids, and constant radius arcs) in rows and segment parameters in columns. These parameters include path length of the segment, east and north positions and heading angle at the beginning of the segment, and the curvature at the beginning and end of the segment.

Map matching. This step uses a Newton-Raphson method to identify the distance along the path s corresponding to the vehicle's current position. This is an iterative method that is initialized with the results from the previous time step. The algorithm estimates the closest point on the path to the current vehicle position by guessing the east and north positions, the heading angle, and the path curvature in an iterative manner. After the closest path point has been identified, the algorithm computes the lateral error e, the heading error $\Delta\Psi$, and the curvature κ of the path point. These values are used in the path following steering controller to keep the vehicle on the desired path.

Path following steering controller. The path following steering controller uses feedforward steering on both the front and rear wheels to approximately follow a path with the given curvature, and lanekeeping feedback on the front wheels only to ensure acceptable path tracking. The controller is based on the work by Kritayakirana and Gerdes (*35*). The steering angles are given by a combination of feedforward and feedback on the front wheels, and feedforward only on the rear wheels.

$$\delta_f = \delta_{f,ffw} + \delta_{f,fb} = \kappa\left(\frac{mb}{LC_f}U_x^2 + \frac{L}{2}\right) - K_{fb}(e + x_{LA}\Delta\Psi)$$
$$\delta_r = \delta_{r,ffw} = \kappa\left(\frac{ma}{LC_r}U_x^2 - \frac{L}{2}\right) \quad (8)$$

The feedforward terms (those multiplying the path curvature κ) are computed by finding the lateral tire forces necessary to track the given path curvature assuming steady-state cornering, with vehicle length L, mass m, front and rear tire cornering stiffnesses C_f and C_r, and vehicle speed U_x. The lanekeeping feedback term in the front steering angle,

based on the work of Rossetter (*36*), combines the lateral error e and heading error $\Delta\Psi$ into a single lookahead error e_{LA} projected at a distance in front of the vehicle x_{LA}, which is multiplied by proportional gain K_{fb}. For this experiment, x_{LA} = 5 m and K_{fb} = 0.052 rad/m.

Speed limiter. The speed is limited to 5 m/s during the return to start phase. The algorithm is straightforward: If the vehicle speed is less than $U_{x,max}$ = 5 m/s, allow the driver to command full motor torque (and thus maximum acceleration); if the speed exceeds $U_{x,max}$, limit the torque to 10% of its maximum value (about 24 N·m). To prevent step changes in commanded torque and reduce switching when the speed is near $U_{x,max}$, we applied a single-pole 0.5-Hz discrete low-pass filter (Eq. 9) to the torque command signal.

$$\tau_{cmd} = \begin{cases} \tau_{des}, & U_x \le U_{x,max} \\ max(\tau_{des}, 0.1\tau_{max}), & U_x > U_{x,max} \end{cases}$$
$$L_1(z) = \frac{6.283 \times 10^{-3}}{z - 0.9937} \quad (9)$$
$$\tau_{cmd,filt} = L_1(z) \times \tau_{cmd}$$

Study participants

The study was conducted with a total of 22 participants with valid driver's licenses. Each participant signed an informed consent form, and we obtained written permission to publish movies S1 and S2. The study protocol and consent form were approved by the Stanford University Institutional Review Board, protocol number 28606. Ten right-handed participants (4 men, 6 women) with mean age 34.9 years experienced the steering ratio perturbation. Twelve participants (6 men, 6 women) with mean age 27 years experienced the steering torque perturbation; one of these participants was left-handed and the remainder were right-handed.

On the basis of the background of the study participants, there is potential for sample bias. For example, the size of the effects in our findings may be sensitive to the age, lifestyle, and driving experience of the participants. Hence, our emphasis is on the process of adaptation rather than on specific quantitative values. The study results as discussed above suggest that the effect of adaptation to altered vehicle handling is important to consider in designing car-to-driver handover.

Statistical analysis

Definition of adaptation metrics

Data analysis was performed with MATLAB (version R2014b, MathWorks), using custom code. The first metric, the steering reversal rate, divides the number of times a driver reverses the direction of the steering wheel through a minimum angle of 0.5° by the total time of the steering maneuver (about 14 s). The first step in computing this metric was to filter the steering angle with a three-pole 100-Hz digital low-pass filter with zero phase shift (using MATLAB's filtfilt function). A custom peak detection algorithm was then used to find the local maxima and minima of the filtered steering angle. The number of steering reversals separated by the minimum 0.5° angle was counted and then divided by the elapsed time.

The second metric, the RMS steering speed, is defined as the derivative of the driver's desired front road wheel angle. The derivative was approximated by taking a first-order finite difference of the steering angle and then filtering with a zero-phase 10-Hz digital low-pass filter. The root mean square of the resulting approximate derivative signal over each entire trial formed the desired metric.

The final metric is defined as the elapsed time between the triggering of the signal light and the next local maximum steering angle. The time corresponding to the activation of the signal light was recorded for each trial and therefore available for use in computation. Using the custom peak detection algorithm on the filtered steering angle from the first metric, the signal light time was subtracted from the time corresponding to the subsequent steering peak. The MATLAB files used to perform this analysis are available as supplementary file downloads.

Statistical methods

Statistical analysis was performed in MATLAB (R2014b) using the Statistics and Machine Learning Toolbox and in Microsoft Excel (version 14.4.2 for Mac 2011). No specific treatment of outliers was performed. Statistical significance was determined using two-sided tests at the α = 0.05 threshold level throughout the paper. Central tendency was estimated using the mean, and all 95% confidence intervals were computed using a t distribution.

For each metric, a one-way repeated-measures analysis of variance (ANOVA) was computed, with trial number as the fixed factor and participant as the repeated measure/random factor. Greenhouse-Geisser ε corrections for lack of sphericity were applied to the ANOVA results. Tables S1 and S2 summarize the ANOVA results. For metrics that showed significant differences in mean according to the ANOVA, post hoc comparisons were made between each pair of trials in Fig. 4. The P values were computed from the t distribution; corrections for multiple comparisons were made by multiplying all P values by 10, the total number of pairwise comparisons (Bonferroni method). After the P values were adjusted, statistically significant results were assessed at the α = 0.05 level. Results of the pairwise comparisons are summarized in table S3. Note that since no metrics for the steering torque modification showed significant differences in ANOVA, post hoc comparisons were not performed for this condition.

SUPPLEMENTARY MATERIALS

robotics.sciencemag.org/cgi/content/full/1/1/eaah5682/DC1
Fig. S1. Steering wheel torque.
Fig. S2. Full steering torque emulator
Fig. S3. Cruise control performance.
Fig. S4. Course.
Fig. S5. Autosteering controller path.
Table S1. ANOVA tables for steering ratio modification.
Table S2. ANOVA tables for steering torque modification.
Table S3. Bonferroni-corrected post hoc comparisons (p_b) for steering ratio modification.
Data files S1 and S2
MATLAB software for data analysis (.zip file)
Movie S1. Automated vehicle returns to the start of the course, with the car controlling the steering and the driver controlling the speed.
Movie S2. Participant reacts to changes in steering ratio: last baseline trial (15:1), first perturbation trial (2:1), last perturbation trial (2:1), and first washout trial (15:1).

REFERENCES AND NOTES

1. SAE On-Road Automated Vehicle Standards Committee, *Taxonomy and Definitions for Terms Related to On-Road Motor Vehicle Automated Driving Systems* (SAE International, 2014).
2. N. Merat, A. H. Jamson, F. C. H. Lai, M. Daly, O. M. J. Carsten, Transition to manual: Driver behaviour when resuming control from a highly automated vehicle. *Tran. Res. Part F Traffic Psychol. Behav.* **27**, 274–282 (2014).
3. B. Mok, M. Johns, K. J. Lee, D. Miller, D. Sirkin, P. Ive, W. Ju, Emergency, automation off: Unstructured transition timing for distracted drivers of automated vehicles, *18th International IEEE Conference on Intelligent Transportation Systems*, Las Palmas de Gran Canaria, Spain, 15 to 18 September 2015 (Institute of Electrical and Electronics Engineers, 2015).

4. A. P. van den Beukel, M. C. van der Voort, The influence of time-criticality on situation awareness when retrieving human control after automated driving, *16th International IEEE Conference on Intelligent Transportation Systems*, The Hague, Netherlands, 6 to 10 October 2013 (Institute of Electrical and Electronics Engineers, 2013).
5. T. E. Trimble, R. Bishop, J. F. Morgan, M. Blanco, *Human Factors Evaluation of Level 2 and Level 3 Automated Driving Concepts: Past Research, State of Automation Technology, and Emerging System Concepts* (National Highway Traffic Safety Administration, 2014).
6. R. Shadmehr, S. Mussa-Ivaldi, *Biological Learning and Control: How the Brain Builds Representations, Predicts Events, and Makes Decisions* (MIT Press, 2012).
7. J. Diedrichsen, R. Shadmehr, R. B. Ivry, The coordination of movement: Optimal feedback control and beyond. *Trends Cognit. Sci.* **14**, 31–39 (2010).
8. J. W. Krakauer, Z. M. Pine, M.-F. Ghilardi, C. Ghez, Learning of visuomotor transformations for vectorial planning of reaching trajectories. *J. Neurosci.* **20**, 8916–8924 (2000).
9. D. M. Wolpert, R. C. Miall, M. Kawato, Internal models in the cerebellum. *Trends Cognit. Sci.* **2**, 338–347 (1998).
10. A. Karniel, Open questions in computational motor control. *J. Integr. Neurosci.* **10**, 385–411 (2011).
11. S. E. Criscimagna-Hemminger, A. J. Bastian, R. Shadmehr, Size of error affects cerebellar contributions to motor learning. *J. Neurophysiol.* **103**, 2275–2284 (2010).
12. K. Wei, K. Körding, Relevance of error: What drives motor adaptation? *J. Neurophysiol.* **101**, 655–664 (2009).
13. K. van der Kooij, E. Brenner, R. J. van Beers, J. B. J. Smeets, Visuomotor adaptation: How forgetting keeps us conservative. *PLOS ONE* **10**, e0117901 (2015).
14. L. N. Gonzalez Castro, A. M. Hadjiosif, M. A. Hemphill, M. A. Smith, Environmental consistency determines the rate of motor adaptation. *Curr. Biol.* **24**, 1050–1061 (2014).
15. D. J. Herzfeld, P. A. Vaswani, M. K. Marko, R. Shadmehr, A memory of errors in sensorimotor learning. *Science* **345**, 1349–1353 (2014).
16. H. G. Wu, Y. R. Miyamoto, L. N. Gonzalez Castro, B. P. Ölveczky, M. A. Smith, Temporal structure of motor variability is dynamically regulated and predicts motor learning ability. *Nat. Neurosci.* **17**, 312–321 (2014).
17. A. Peled, A. Karniel, Knowledge of performance is insufficient for implicit visuomotor rotation adaptation. *J. Mot. Behav.* **44**, 185–194 (2012).
18. R. Schween, W. Taube, A. Gollhofer, C. Leukel, Online and post-trial feedback differentially affect implicit adaptation to a visuomotor rotation. *Exp. Brain Res.* **232**, 3007–3013 (2014).
19. H. G. Wu, M. A. Smith, The generalization of visuomotor learning to untrained movements and movement sequences based on movement vector and goal location remapping. *J. Neurosci.* **33**, 10772–10789 (2013).
20. J. B. Brayanov, D. Z. Press, M. A. Smith, Motor memory is encoded as a gain-field combination of intrinsic and extrinsic action representations. *J. Neurosci.* **32**, 14951–14965 (2012).
21. M. F. Rotella, I. Nisky, M. Koehler, M. D. Rinderknecht, A. J. Bastian, A. M. Okamura, Learning and generalization in an isometric visuomotor task. *J. Neurophysiol.* **113**, 1873–1884 (2015).
22. J. W. Krakauer, P. Mazzoni, Human sensorimotor learning: Adaptation, skill, and beyond. *Curr. Opin. Neurobiol.* **21**, 636–644 (2011).
23. D. M. Wolpert, J. Diedrichsen, J. R. Flanagan, Principles of sensorimotor learning. *Nat. Rev. Neurosci.* **12**, 739–751 (2011).
24. C. C. Macadam, Understanding and modeling the human driver. *Veh. Syst. Dyn.* **40**, 101–134 (2003).
25. W. A. MacDonald, E. R. Hoffmann, Review of relationships between steering wheel reversal rate and driving task demand. *Hum. Factors* **22**, 733–739 (1980).
26. B. L. Benson, J. A. Anguera, R. D. Seidler, A spatial explicit strategy reduces error but interferes with sensorimotor adaptation. *J. Neurophysiol.* **105**, 2843–2851 (2011).
27. R. Shadmehr, F. A. Mussa-Ivaldi, Adaptive representation of dynamics during learning of a motor task. *J. Neurosci.* **14**, 3208–3224 (1994).
28. E. Burdet, R. Osu, D. W. Franklin, T. E. Milner, M. Kawato, The central nervous system stabilizes unstable dynamics by learning optimal impedance. *Nature* **414**, 446–449 (2001).
29. A. J. Pick, D. J. Cole, Neuromuscular dynamics in the driver–vehicle system. *Veh. Syst. Dyn.* **44**, 624–631 (2006).
30. A. J. Pick, D. J. Cole, Driver steering and muscle activity during a lane-change manoeuvre. *Veh. Syst. Dyn.* **45**, 781–505 (2007).
31. A. J. Pick, D. J. Cole, A mathematical model of driver steering control including neuromuscular dynamics. *J. Dyn. Sys. Meas. Control.* **130**, 031004 (2008).
32. D. A. Abbink, M. Mulder, E. R. Boer, Haptic shared control: Smoothly shifting control authority? *Cognit. Technol. Work* **14**, 19–28 (2012).
33. A. Balachandran, J. C. Gerdes, Designing steering feel for steer-by-wire vehicles using objective measures. *IEEE/ASME Trans. Mechatronics* **20**, 373–383 (2015).
34. P. A. Theodosis, J. C. Gerdes, Generating a racing line for an autonomous racecar using professional driving techniques, *ASME 2011 Dynamic Systems and Control Conference*, Arlington, TX, 31 October to 2 November 2011 (Dynamic Systems and Control Division, 2011).
35. K. Kritayakirana, J. C. Gerdes, Autonomous vehicle control at the limits of handling. *Int. J. Veh. Auton. Syst.* **10**, 271–296 (2012).
36. E. J. Rosseter, J. C. Gerdes, A study of lateral vehicle control under a 'virtual' force framework, *6th International Symposium on Advanced Vehicle Control*, Hiroshima, Japan, 9 to 13 September 2002 (Advanced Vehicle Control, 2002).
37. C. G. Bobier, J. C. Gerdes, Steer-by-wire suspension design: Geometries to enhance peak tire force estimation, *21st International Symposium on Dynamics of Vehicles on Roads and Tracks*, Stockholm, Sweden, 17 to 21 August 2009 (International Association for Vehicle System Dynamics, 2009).

Acknowledgments: We thank M. Brown and L. Mondavi for experimental support, G. Zhang for technical support with X1, S. Russell for photography, and members of the Dynamic Design Lab for intellectual discussion and technical help. **Funding:** H.E.B.R., L.K.H., S.P., and J.C.G. are supported by the Revs Program at Stanford University, and H.E.B.R., L.K.H., and J.C.G. are supported in part by the Toyota Class Action Settlement Safety Research and Education Program (the conclusions being expressed are the authors' only and have not been sponsored, approved, or endorsed by Toyota or Plaintiffs' Class Counsel). I.N. is supported by the Israeli Science Foundation (grant number 823/15) and by the Helmsley Charitable Trust through the Agricultural, Biological and Cognitive Robotics Initiative of Ben-Gurion University of the Negev. A.M.O. is supported by the U.S. NSF (grant number 1227406). **Author contributions:** H.E.B.R., L.K.H., and I.N. designed and performed all experiments, analyzed data, interpreted the results, and wrote the paper. S.P. performed experiments and wrote the paper. A.M.O. and J.C.G. designed experiments, interpreted results, and wrote the paper. **Competing interests:** H.E.B.R. is currently an autonomous driving researcher with Renault Innovation Silicon Valley in Sunnyvale, CA. **Data and materials availability:** Data are available as Supplementary Materials: data files S1 and S2.

Submitted 14 July 2016
Accepted 19 October 2016
Published 6 December 2016
10.1126/scirobotics.aah5682

Citation: H. E. B. Russell, L. K. Harbott, I. Nisky, S. Pan, A. M. Okamura, J. C. Gerdes, Motor learning affects car-to-driver handover in automated vehicles. *Sci. Robot.* **1**, eaah5682 (2016).

Science Robotics

Motor learning affects car-to-driver handover in automated vehicles

Holly E. B. Russell, Lene K. Harbott, Ilana Nisky, Selina Pan, Allison M. Okamura, and J. Christian Gerdes

Sci. Robot. **1** (1), eaah5682. DOI: 10.1126/scirobotics.aah5682

Science Robotics (ISSN 2470-9476) is published by the American Association for the Advancement of Science. 1200 New York Avenue NW, Washington, DC 20005. The title *Science Robotics* is a registered trademark of AAAS.